Original Research

Noninvasive Magnetic Resonance Imaging Evaluation of Cerebral Blood Flow With Acetazolamide Challenge in Patients With Cerebrovascular Stenosis

John A. Detre, MD,[1,2]* Owen B. Samuels, MD,[1] David C. Alsop, PhD,[2] Julio B. Gonzalez-At, PhD,[1] Scott E. Kasner, MD,[1] and Eric C. Raps, MD[1]

To evaluate the utility of using magnetic resonance imaging (MRI) of cerebral blood flow (CBF) in conjunction with pharmacologic flow augmentation, the authors imaged 14 patients with ischemic symptoms referable to large artery cerebrovascular stenosis of the anterior circulation. CBF was measured by using continuous arterial spin labeling (CASL) both at rest and 10 minutes after 1 g intravenous acetazolamide on a commercial 1.5 Tesla scanner. Quantitative CBF images were calculated along with augmentation images showing the effects of acetazolamide. Interpretable studies were obtained from all patients. Based on the image data as well as a region of interest analysis of CBF changes in middle cerebral artery distributions, varying patterns of augmentation were observed that suggested differing mechanisms of ischemic symptomatology. The ability to obtain this information in conjunction with a structural MRI examination extends the diagnostic potential for MRI in cerebrovascular disease and allows the value of augmentation testing in clinical management to be assessed more widely. J. Magn. Reson. Imaging 1999;10: 870–875. © **1999 Wiley-Liss, Inc.**

Index terms: acetazolamide; cerebral blood flow; cerebrovascular disease; magnetic resonance imaging; ischemia

MAGNETIC RESONANCE IMAGING (MRI) has provided unprecedented image resolution for structural brain imaging and is now used widely in the assessment of cerebrovascular disorders. In addition, magnetic resonance angiography (MRA) can assess large-vessel patency with accuracy approaching that of angiography (1–3). Recently, a variety of methods have been developed that allow hemodynamic measurement of brain parenchymal perfusion using magnetic resonance. These methods include visualization of the first-pass or volume distribution of exogenous contrast (4) and the use of endogenous contrast in the form of electromagnetically labeled arterial water, arterial spin labeling (ASL) (5,6). ASL techniques are divided into pulsed ASL and continuous ASL (CASL) approaches. In both cases, electromagnetically labeled arterial water serves as a freely diffusible perfusion tracer that can be used to measure classical tissue perfusion ($ml \cdot 100\ g^{-1} \cdot min^{-1}$). The principal difference between the ^{1}H ASL tracer and ^{15}O tracers used in positron emission tomography (PET) is the very short half-life of the ASL tracer, which decays with the relaxation parameter T1. Nonetheless, due to the high sensitivity of ^{1}H-MRI, tissue signal changes due to perfusion with the ASL tracer can be measured reliably. Although pulsed ASL is methodologically easier to implement, continuous ASL provides greater perfusion contrast (7) and more direct quantification (8) through modification of the Bloch equations to include perfusion effects of CASL. Modifications to the data-acquisition protocol also have rendered the CASL method relatively insensitive to arterial transit time delays (8).

CASL perfusion MRI can provide high-resolution cerebral blood flow (CBF) images that were obtainable previously only by imaging exogenously administered diffusible tracers, such as ^{15}O in PET scanning or x-ray computed tomography with Xenon contrast. In addition, CASL MRI recently has been extended to a multislice examination (9), which is critical for clinical use and which can be obtained in a timely fashion in conjunction with routine anatomic MRI scanning. CBF values obtained using CASL MRI have been validated against microsphere CBF in animal models (10) and against PET CBF measurements in humans (11).

CBF is maintained over a broad range of perfusion pressures through cerebrovascular autoregulation (12). Because autoregulatory vasodilatation can maintain CBF, it has been suggested that CBF alone is an inadequate measure of hemodynamic compromise (13). Although resting reductions in CBF clearly are abnormal, alterations in hemodynamic reserve also are significant, because they suggest that the autoregulatory

[1]Department of Neurology, University of Pennsylvania Medical Center, Philadelphia, PA 19104.

[2]Department of Radiology, University of Pennsylvania Medical Center, Philadelphia, PA 19104.

Contract grant sponsor: National Institutes of Health; Contract grant numbers: NS01668 and NS02079; Contract grant sponsor: American Heart Association; Contract grant sponsor: The Whitaker Foundation.

*Address reprint requests to: J.A.D., Department of Neurology, University of Pennsylvania Medical Center, 3400 Spruce Street, Philadelphia, PA 19104. E-mail: detre@mail.med.upenn.edu

Received April 29, 1999; Accepted July 22, 1999.

capacity of the cerebral vasculature may be nearly exhausted. In the absence of intact autoregulation, CBF becomes dependent on arterial blood pressure. This mechanistic consideration is the basis for withholding antihypertensive therapy in acute stroke, in which cerebrovascular autoregulation is known to be impaired; however, its significance in chronic cerebrovascular disease remains uncertain.

Cerebrovascular reserve can be assessed by using a variety of methods, including measurement of oxygen extraction and/or blood flow/blood volume ratios by PET scanning and measurement of hemodynamic responses to pharmacologic flow augmentation with carbon dioxide or acetazolamide using a variety of flow-sensitive methods, such as PET, single-photon emission computed tomography (SPECT), transcranial Doppler, Xenon-enhanced computed tomography (CT) scanning, or MRI. Several recent studies of cerebrovascular reserve testing have demonstrated its potential utility in predicting subsequent stroke (14–16), although other studies have obtained conflicting results (13,17). In asymptomatic patients with cerebrovascular risk factors, a decreased vasodilatory response to acetazolamide was found to correlate with the extent of subcortical ischemic change (18).

We have previously demonstrated that CASL MRI can detect resting CBF defects in patients with symptomatic cerebrovascular disease (19). It also should provide a convenient method for measuring quantitatively and noninvasively the effects of pharmacologic flow augmentation. The objective in this study was to extend our observations of cerebral hemodynamics using CASL MRI to evaluate cerebrovascular reserve by using an acetazolamide challenge in a small cohort of patients with symptomatic, large-artery cerebrovascular disease.

MATERIALS AND METHODS

Fourteen consecutively recruited consenting patients with symptomatic, anterior circulation, large-artery stenosis were studied using a protocol approved by the University of Pennsylvania Institutional Review Board. Patients in whom stenosis of the extracranial or intracranial internal carotid artery and/or middle cerebral arteries was diagnosed during routine clinical evaluation and in whom structural MRI did not reveal large (>10% of hemispheric volume) infarcts were included. Evaluation of arterial stenosis was based on results of carotid Doppler, MRA, and/or digital subtraction angiography (DSA) carried out as part of routine clinical evaluation.

Imaging was performed on a standard GE Horizon Echospeed 1.5-Tesla MRI scanner (GE Medical Systems, Milwaukee WI) using the product quadrature head coil and foam padding to restrict head motion comfortably. All patients underwent routine T1-weighted spin-echo and T2-weighted fast spin-echo (FSE) or fluid-inverted (FLAIR) fast spin-echo imaging. CASL perfusion MRI was then performed as described previously (8,9,) with a labeling gradient of 0.25 G/cm, a labeling radiofrequency (RF) of 35 mG, temporal interleaving of labeled and control images, a TR of 4 seconds, and a nominal postlabeling delay of 1.5 seconds. The postlabeling delay reduces the sensitivity of the perfusion image to the transit time from the labeling plane and strongly attenuates the contribution of intraluminal arterial spins to the image intensity. CASL was performed at the cervicomedullary junction using velocity-driven adiabatic inversion with an amplitude-modulated control labeling pulse (9), which reproduces the frequency-dependent off-resonance effects of the labeling pulse and therefore permits multislice imaging.

The effects of CASL were measured by using single-shot, gradient-echo, echoplanar images with a field of view of 24 cm along the frequency-encoding direction, 15 cm for the phase direction, and an acquisition matrix of 64×40, resulting in an in-plane resolution of 3.75 mm^2. An acquisition bandwidth of ± 62.5 kHz allowed an effective TE of 22 msec and an image acquisition time of 60 msec. Multislice image acquisition was performed without pausing between slices, so that 8 slices could be acquired in less than 500 msec. Because each slice is acquired at a slightly different time, the actual postlabeling delay varies from 1.5 seconds to 1.98 seconds. Slice thickness was 8 mm, with interslice gaps of 2 mm. Temporal interleaving of 45 ASL and 45 control images were employed for a total acquisition time of approximately 6 minutes. CASL perfusion MRI was performed both at baseline and at 10 minutes after administration of 1 gram of intravenous acetazolamide. Prior to the first CBF scan, multislice, echoplanar T1 mapping scans were performed for quantification of the CBF images along with the acquisition of data used to correct static magnetic field inhomogeneities as described previously (8). The total imaging time for these preparatory sequences was 3 minutes.

Raw echo amplitudes from echoplanar images were saved and transferred to a workstation for reconstruction and processing using software written in IDL (Research Systems, Boulder, CO). A correction for image distortion and alternate k-space line errors was performed on each image by using data acquired during a phase-encoded reference scan (20). A side effect of this correction is that image regions in which insufficient signal is present to measure the frequency offset are set to zero. An algorithm to remove subtle motion artifacts from the images (21) also was performed on the individual images prior to signal averaging. Quantitative CBF images were calculated as described previously (8), interpolated from the original 40×64 matrix to an 80×128 matrix, and smoothed in-plane by using a 0.5-pixel, full-width, half-maximum (FWHM) Gaussian kernel.

Maps of percent acetazolamide augmentation were obtained by dividing the difference between the postacetazolamide and the preacetazolamide CBF images by the preacetazolamide image after smoothing in three dimensions using a truncated Gaussian kernel equivalent to 4.7 pixels FWHM in plane and 1.8 pixels through plane (corresponding to the nominal 3.75 mm resolution in plane and 10 mm resolution through plane). This additional smoothing was used to reduce motion effects between preacetazolamide and postacetazolamide scans that were not eliminated by the motion-correction algorithm. Regions of interest representing the right and left

middle cerebral artery (MCA) distributions were drawn manually on the CBF images from published templates of vascular anatomy (22) and were used to extract CBF changes in this distribution with acetazolamide.

RESULTS

Table 1 provides clinical information and significant vascular anatomy from each of the 14 patients in this study and summarizes the results of perfusion imaging. Locations of vascular lesions were unilateral cervical carotid stenosis (>70%; $N = 4$), tandem carotid stenosis (carotid bifurcation and carotid siphon stenosis; $N = 2$), carotid siphon stenosis alone ($N = 1$), and middle cerebral stenosis ($N = 7$). Neurologic symptoms were referable to the diseased vascular anatomy in all patients. All but one patient (patient 1) had MRI evidence of cerebral ischemic changes.

Interpretable CBF images were obtained from all patients both before and after acetazolamide administration. Qualitative descriptions of baseline and postacetazolamide perfusion maps are described briefly in Table 1. In patients with cortical infarcts, corresponding hypoperfusion was observed on resting perfusion maps. Perfusion maps in several patients showed bright, linear features indicative of arterial transit times in excess of 1.5 seconds (19). These effects typically were focal, occurring in the most affected vascular distribution, although, in patient 14, diffuse transit effects were observed.

Qualitative descriptions of the effects of acetazolamide augmentation also are provided in Table 1. A variety of effects were observed. Several patients failed to increase CBF in response to acetazolamide. This occurred in several patterns, including diffuse augmentation failure (patients 1, 9, and 13), patchy augmentation failure (patient 14), or focal augmentation failure corresponding to the vascular distributions of proximal stenoses (patients 1, 8, 10, and 18). Four patients showed CBF augmentation throughout the brain except in regions of infarct (patients 2, 3, 5, and 12). In two patients, this augmentation was quite marked (patients 4 and 11).

Table 2 provides the results of CASL MRI perfusion measurements in MCA territories. Because all patients had cerebrovascular disease affecting the anterior circu-

Table 1
Patient Demographics, Clinical Data, and Perfusion Results*

Patient	Age (years)/ gender	Affected hemisphere	Clinical history	Structural MRI lesion	Vascular anatomy	Perfusion MRI (baseline)	Perfusion MRI (augmentation)
1	59/M	R	Recurrent L-HP, L-HS	None	Severe R-MCA stenosis (MRA)	Normal; R-MCA transit artifact	Focal decrement L-MCA
2	83/M	R	Recurrent L-HP, L-HS	Post. div. R-MCA (cort.)	Mild R-MCA stenosis (MRA)	Focal hypoperfusion R-MCA	Normal (except in infarct)
3	69/M	R > L	LH, ataxia	B (subcort. only)	Mod. R > L-MCA stenosis (MRA)	Global and patchy focal hypoperfusion	Patchy
4	50/M	L	Recurrent L-HP, L-HS	Post. div. R-MCA (cort.)	Mild R-MCA stenosis (MRA)	Global and focal post. div. R-MCA hypoperfusion	Hyperaugmentation (except in infarct)
5	76/M	L	Recurrent aphasia R-HP, R-HS	Post. div. and BZ L-MCA	Mod. L-MCA stenosis (MRA)	Focal hypoperfusion L-MCA	Normal (except in infarct)
6	64/M	L	Recurrent R-HP (hand only)	L > R subcort.	Mod. L-ICA and intracranial stenosis (DSA)	Focal hypoperfusion R-MCA; L-MCA transit artifact	Diffuse decrement
7	62/M	L > R	Aphasia, R-HP, R-HS	Post. div L-MCA (subcort.)	L-ICA occl., severe R-ICA stenosis (MRA)	Focal hypoperfusion L-MCA; B transit artifact	Patchy augmentation
8	64/F	L	Recurrent R-HP, R-HS, aphasia	Ant. div. and BZ L-MCA (subcort.)	Severe L-siphon stenosis (DSA)	Focal hypoperfusion L-MCA; L-MCA transit artifact	Focal decrement L-MCA
9	77/M	R > L	Ataxia	B subcort.	Severe R-ICA and mod. L-ICA stenosis (DSA)	Hypoperfusion ant. circulation	Poor ant. circulation
10	47/M	L	Recurrent R-HP, R-HS aphasia	L-MCA (cort.)	Mod. L-ICA and siphon stenosis (MRA)	Grossly symmetrical; L-MCA transit artifact	Decrement L hemisphere
11	52/M	L	Recurrent R-HP, R-HS, aphasia	L-MCA (subcort.)	Severe L-ICA stenosis (MRA)	Global hypoperfusion; L-MCA transit artifact	Hyperaugmentation
12	62/F	L	Recurrent R-HP, R-HS, aphasia	Post div. L-MCA (cort.), B subcort.	Severe L-MCA stenosis (DSA)	Focal hypoperfusion post. div. L-MCA	Normal
13	52/F	L > R	Recurrent R-HP, aphasia	L-MCA (subcort.)	L-ICA occl., R intracranial stenosis (MRA)	Diffuse hypoperfusion; diffuse transit artifact	Diffuse decrement
14	61/F	L	Recurrent cognitive changes	L-MCA	Severe L-MCA stenosis (DSA)	Hypoperfusion L-MCA; transit artifact L-MCA	Patchy focal decrement

*M = male; F = female; R = right; L = left; B = bilateral; BZ = border zone; HP = hemiparesis; HS = hemisensory loss; ant. = anterior; post. = posterior; div. = division; cort. = cortical; subcort. = subcortical; mod. = moderate; ICA = internal carotid artery; MCA = middle cerebral artery; MRI = magnetic resonance imaging; MRA = magnetic resonance angiography; DSA = digital subtraction angiography; occl. = occlusion; art. = artifact.

Table 2
Flow Values in Middle Cerebral Artery Distributions†

Patient	Affected hemisphere	Affected hemisphere CBF[a]		Unaffected hemisphere CBF[a]		% Change affected	% Change unaffected	% Change total MCA
		Baseline	Acetazolamide	Baseline	Acetazolamide			
6	L	34	38	38	26	12	−33	−10
13	R	95	86	91	83	−9	−9	−9
9	R	34	37	42	47	10	11	11
1	R	62	59	60	76	−5	27	11
10	L	73	81	69	80	12	17	14
8	L	41	44	46	59	6	29	18
14	L	54	76	43	50	41	15	28
2	R	60	86	61	81	43	33	38
3	R	27	38	28	40	43	42	42
7	L	31	44	44	65	42	48	45
12	L	48	71	52	82	48	58	53
5	L	35	52	51	81	49	60	54
11	L	45	91	43	79	102	85	94
4	R	21	55	35	71	164	103	133
Mean		47	61*	50	66**	40	35	37

†Patients are sorted by % change after acetazolamide in the affected middle cerebral artery (MCA) distribution.
[a]Cerebral blood flow (CBF) values are expressed in units of ml · 100 g^{-1} · min^{-1}.
*$P = 0.004$ vs. baseline flow values.
**$P = 0.002$ vs. baseline flow values.

lation, this territory was chosen for comparison, although hemispheric values showed similar trends. CBF values before and after acetazolamide as well as the percent change in CBF after acetazolamide administration are shown. In Table 2, patient results are sorted by the average percent change in both MCA regions, ranging from lowest to highest. Although there was considerable variability in the CBF responses to acetazolamide, particularly in the affected hemisphere, statistically significant increases in CBF were observed in both the affected and unaffected hemispheres for the group.

Considering the various distributions of acetazolamide effects observed in the context of the available clinical information, it was possible to characterize several response types suggesting the presence or absence of hemodynamic impairment. A number of patients failed to increase CBF in response to acetazolamide. Patients with diffuse augmentation failure (patients 1, 9, and 13) had widespread occlusive vascular disease, and structural imaging showed primarily subcortical ischemic changes consistent with an internal border-zone distribution of ischemia (23–25). Fig. 1 (top) shows T2-weighted images and the augmentation map acquired from patient 9, who had bilateral carotid stenosis and minimal CBF change in the carotid distributions after acetazolamide. Structural MRI in this patient showed bilateral subcortical ischemic changes consistent with hypoperfusion in the anterior circulation distribution. This patient presented with symptoms of recurrent ataxia, which ultimately were attributed to a pseudovertebrobasilar syndrome (26). The finding of normal augmentation in the posterior circulation supports this diagnosis.

Several patients showed patchy augmentation failure (patient 14) or focal augmentation failure corresponding to the vascular distributions of proximal stenoses (patients 1, 8, 10, and 18). Fig. 1 (middle) shows images acquired from patient 1, who had right MCA stenosis and a focal augmentation deficit in this distribution after acetazolamide. The resting CBF image also shows effects of a prolonged arterial transit time (19). Structural MRI was negative. This patient presented with recurrent episodes of left hemiparesis and hemisensory loss consistent with impaired cerebrovascular reserve in the right MCA distribution. Although the augmentation map shows reduced CBF in this distribution after acetazolamide, the patient did not become symptomatic during the study.

Four patients showed robust CBF augmentation throughout the brain despite proximal arterial stenoses, except in regions of infarct (patients 2, 3, 5, and 12). In two patients, this augmentation was quite marked (patients 4 and 11). Fig. 1 (bottom) shows results obtained from patient 4, who had a right MCA stenosis and relatively low arterial blood pressure. Resting CBF was diffusely low in this patient, but there was very marked augmentation after acetazolamide, with CBF changes of up to 200% of baseline, including the right MCA distribution. In this case, we postulate that the blood pressure range for autoregulation had been shifted upward due to chronic hypertension and that low resting CBF was attributable to a baseline blood pressure that was below the autoregulatory range rather than to exceeding autoregulatory capacity distal to an intracranial stenosis.

DISCUSSION

The primary goal of this study was to evaluate the feasibility of CASL MRI with acetazolamide challenge to assess cerebrovascular reserve in patients with large artery cerebrovascular occlusive disease. The imaging protocol was well tolerated and was readily combined with a routine clinical MRI examination. CASL MRI was able both to quantify baseline CBF and to assess cerebrovascular reserve using acetazolamide augmentation. In combination with MRA, this allows a complete hemodynamic and structural assessment to be made

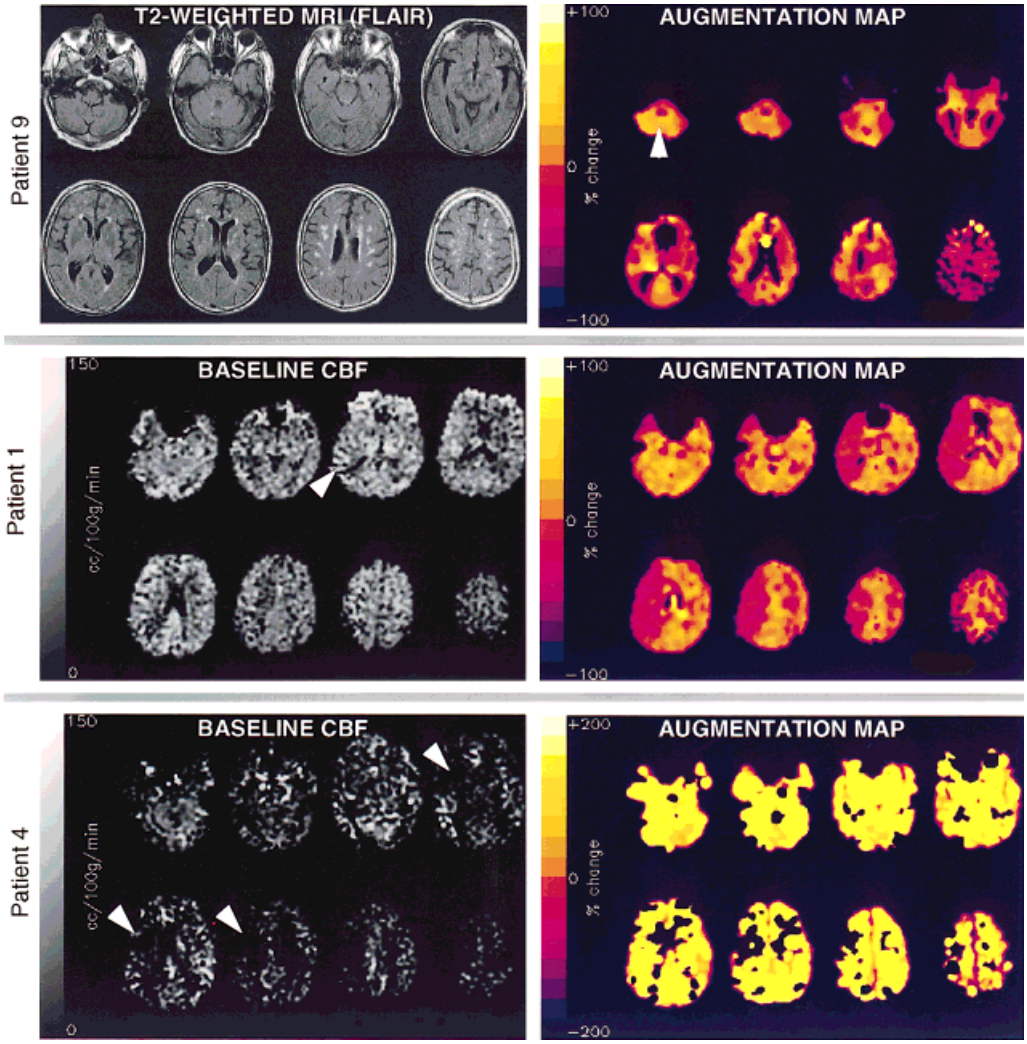

Figure 1. Examples of image data acquired using continuous arterial spin labeling (CASL) perfusion magnetic resonance imaging (MRI) with acetazolamide. **Top:** Data acquired from patient 9. On the left, T2-weighted, fluid-attenuated inversion recovery (FLAIR) images show subcortical ischemic changes in the anterior circulation distributions bilaterally. On the right, the augmentation map clearly shows minimal change in cerebral blood blow (CBF) in the anterior circulation, with the most pronounced augmentation in the posterior circulation distribution (arrowhead). The color scale shows the percent CBF change ranging from −100% to 100% of resting values. **Middle:** Data acquired from patient 1. On the left, the resting CBF appears grossly symmetrical, although linear hyperintensities suggesting delayed arterial transit are evident (arrowhead). The gray scale shows CBF values ranging from 0 ml · 100 g^{-1} · min^{-1} to 150 ml · 100 g^{-1} · min^{-1}. On the right, the augmentation map demonstrates an augmentation deficit in the right middle cerebral artery (MCA) distribution. The color scale shows percent flow change ranging from −100% to 100% of resting values. **Bottom:** Data acquired from patient 4. On the left, the resting CBF is very low throughout, with a deficit in the right anterior MCA distribution corresponding to the location of an anterior MCA infarct (arrowheads). The gray scale shows CBF values ranging from 0 ml · 100 g^{-1} · $min^{-1}$to 150 ml · 100 g^{-1} · min^{-1}. On the right, the augmentation map demonstrates a marked CBF increase, except in the region of prior infarction. The color scale shows percent flow change ranging from −200% to 200% of resting values.

using a single modality, without requiring repeated doses of intravenous contrast (27).

In the small cohort of patients studied here, CASL MRI with acetazolamide augmentation revealed varying patterns of CBF change, suggesting differing etiologies of ischemic symptomatology that ultimately may be used to guide further diagnostic evaluation and therapeutic intervention. For example, in patients presenting with focal intracranial stenosis, the presence of an augmentation deficit in that vascular distribution would support the notion of hemodynamic compromise specifically due to the lesion, whereas the absence of an augmentation deficit would suggest that there may be another etiology for symptoms, such as cardiac or carotid embolism. Similarly, patients with unexpectedly robust global augmentation may have insufficient cardiac output as their primary cause of symptoms, despite the presence of stenotic lesions. Given the small number of highly selected patients studied, these findings and their clinical implications must be taken as preliminary and need to be validated in a larger, prospectively recruited series.

Nearly all cohorts of patients undergoing cerebrovascular reserve testing include some patients in whom

flow decreases in the distribution of a stenotic artery after acetazolamide administration, presumably due to a "steal" phenomenon (28). In rare cases, this has been associated with transient neurologic symptoms (17,29). In patients with focal augmentation deficits in the distribution of proximal arterial stenoses, resting CBF images typically showed evidence of prolonged arterial transit times in the vascular distribution of the augmentation deficit (as described in Fig. 1, middle), suggesting the possibility that arterial transit time measurement may provide an alternate means for screening hemodynamically significant stenoses and would avoid the potential risks of acetazolamide administration. In another small series of patients, a reduction of CBF after acetazolamide was associated with delayed arterial supply via leptomeningeal collaterals (30), which is the likely mechanism for transit effects observed in CASL perfusion imaging. However, transit artifact in resting perfusion images also was observed in patients with other augmentation patterns and therefore is not uniquely equivalent to augmentation failure. The possibility of generating maps representing arterial transit time is a capability of ASL techniques due to the extremely short half-life of the spin label, and this is an area for future technical development.

In conclusion, CASL MRI is a noninvasive method that rapidly provides high-resolution images of CBF and can be combined successfully with augmentation testing. Although the value of augmentation testing for predicting patient outcome or guiding clinical management remains controversial (31), differing patterns of hemodynamic change suggesting differing etiologies are clearly elucidated by this procedure. The ability to obtain this information inexpensively and noninvasively during a structural MRI examination extends the diagnostic potential for this modality and allows the value of augmentation testing for clinical management to be assessed more widely.

REFERENCES

1. Blakeley DD, Oddone EZ, Hasselblad V, Simel DL, Matchar DB. Noninvasive carotid artery testing. A meta-analytic review. Ann Int Med 1995;122:360–367.
2. Dagirmanjian A, Ross JS, Obuchowski N, et al. High resolution, magnetization transfer saturation, variable flip angle, time-of-flight MRA in the detection of intracranial vascular stenoses. J Comp Assist Tomogr 1995;19:700–706.
3. Turnipseed WD, Kennell TW, Turski PA, Acher CW, Hoch JR. Combined use of duplex imaging and magnetic resonance angiography for evaluation of patients with symptomatic ipsilateral high-grade carotid stenosis. J Vasc Surg 1993;17:832–839.
4. Rosen BR, Belliveau JW, Chien D. Perfusion imaging by nuclear magnetic resonance. Magn Reson Q 1989;5:263–281.
5. Detre JA, Zhang W, Roberts DA, et al. Tissue specific perfusion imaging using arterial spin labeling. NMR Biomed 1994;7:75–82.
6. Edelman RR, Siewert B, Darby DG, et al. Qualitative mapping of cerebral blood flow and functional localization with echo-planar MR imaging and signal targeting with alternating radio frequency. Radiology 1994;192:513–520.
7. Wong EC, Buxton RB, Frank LR. A theoretical and experimental comparison of continuous and pulsed arterial spin labeling techniques for quantitative perfusion imaging. Magn Reson Med 1998; 40:348–355.
8. Alsop DC, Detre JA. Reduced transit-time sensitivity in noninvasive magnetic resonance imaging of human cerebral blood flow. J Cereb Blood Flow Metabol 1996;16:1236–1249.
9. Alsop DC, Detre JA. Multisection cerebral blood flow MR imaging with continuous arterial spin labeling. Radiology 1998;208:410–416.
10. Walsh EG, Minematsu K, Leppo J, Moore SC. Radioactive microsphere validation of a volume localized continuous saturation perfusion measurement. Magn Reson Med 1993;31:147–153.
11. Ye FQ, Berman KF, Ellmore T, et al. H2^{15}O PET validation of arterial spin tagging measurements of cerebral blood flow in humans [abstract]. Proc Intl Magn Reson Med 1997;5:87.
12. Lassen NA. Control of cerebral circulation in health and disease. Circ Res 1974;34:749–760.
13. Powers WJ. Cerebral hemodynamics in ischemic cerebrovascular disease. Ann Neurol 1991;29:231–240.
14. Kuroda S, Kamiyama H, Abe H, Houkin K, Isobe M, Mitsumori K. Acetazolamide test in detecting reduced cerebral perfusion reserve and predicting long-term prognosis in patients with internal carotid artery occlusion. Neurosurgery 1993;32:912–918.
15. Gur AY, Bova I, Bornstein NM. Is impaired cerebral vasomotor reactivity a predictive factor of stroke in asymptomatic patients? Stroke 1996;27:2188–2190.
16. Webster MW, Makaroun MS, Steed DL, Smith HA, Johnson DW, Yonas H. Compromised cerebral blood flow reactivity is a predictor of stroke in patients with symptomatic carotid artery occlusive disease. J Vasc Surg 1995;21:338–344.
17. Yokota C, Hasegawa Y, Minematsu K, Yamaguchi T. Effect of acetazolamide reactivity and long-term outcome in patients with major cerebral artery occlusive diseases. Stroke 1998;29:640–644.
18. Isaka Y, Okamoto M, Ashida K, Imaizumi M. Decreased cerebrovascular dilatory capacity in subjects with asymptomatic periventricular hyperintensities. Stroke 1994;25:375–381.
19. Detre JA, Alsop DC, Vives LR, Maccotta L, Teener JW, Raps EC. Noninvasive MRI evaluation of cerebral blood flow in cerebrovascular disease. Neurology 1998;50:633–641.
20. Alsop DC. Correction of ghost artifacts and distortion in echo-planar MR imaging with an iterative reconstruction technique [abstract]. Radiology 1995;197P:388.
21. Alsop DC, Detre JA. Reduction of excess noise in fMRI time series data using noise image templates [abstract]. Proc Intl Magn Reson Med 1997;5:1687.
22. Matsui T, Hirano A. An atlas of the human brain for computerized tomography. Tokyo: Igaku-Shoin; 1978.
23. Moody DM, Bell MA, Challa VR. Features of the cerebral vascular pattern that predict vulnerability to perfusion or oxygenation deficiency: an anatomic study. AJNR 1990;11:431–439.
24. de Reuck J. The human periventricular arterial blood supply and the anatomy of cerebral infarctions. Eur Neurol 1971;5:321–334.
25. Weiller C, Ringelstein E, Reiche W, Buell U. Clinical and hemodynamic aspects of low-flow infarcts. Stroke 1991;22:1117–1123.
26. Fisher M, McQuillen JB. Bilateral cortical borderzone infarction: a pseudobrainstem stroke. Arch Neurol 1981;38:62–63.
27. Guckel FJ, Brix G, Schmiedek P, et al. Cerebrovascular reserve capacity in patients with occlusive cerebrovascular disease: assessment with dynamic susceptibility contrast-enhanced MR imaging and the acetazolamide stimulation test. Radiology 1996;201:405–412.
28. Strandgaard S, Paulson OB. Pathophysiology of stroke. J Cardiovasc Pharmacol 1990;15:S38–S42.
29. Kuwabara Y, Ichiya Y, Sasaki M, Yoshida T, Masuda K. Time dependency of the acetazolamide effect on cerebral hemodynamics in patients with chronic occlusive cerebral arteries. Early steal phenomenon demonstrated by [^{15}O]H2O positron emission tomography. Stroke 1995;26:1825–1829.
30. Smith HA, Thompson-Dobkin J, Yonas H, Flint E. Correlation of xenon-enhanced computed tomography-defined cerebral blood flow reactivity and collateral flow patterns. Stroke 1994;25:1784–1787.
31. Barnett HJM. Hemodynamic cerebral ischemia: an appeal for systematic data gathering prior to a new EC/IC trial. Stroke 1997;28:1857–1860.